Rapamycin inhibits B16 melanoma cell viability *in vitro* and *in vivo* by inducing autophagy and inhibiting the mTOR/p70-S6k pathway

PENGHUI WANG[1*], HAIFANG ZHANG[2*], KAIKAI GUO[1], CHUN LIU[2], SHIMIN CHEN[1], BAOPENG PU[1], SIRUN CHEN[3], TONG FENG[4], HANYI JIAO[1] and CHANG GAO[1]

[1]Department of Basic Medicine and Life Sciences, Hainan Medical University, Haikou, Hainan 570100; [2]Hainan Institute for Drug Control, Haikou, Hainan 570216; [3]Hainan Medical University Press; [4]School of Pharmacy, Hainan Medical University, Haikou, Hainan 570100, P.R. China

Received September 15, 2023; Accepted January 19, 2024

DOI: 10.3892/ol.2024.14273

Abstract. Rapamycin is an immunosuppressant that has been shown to prevent tumor growth following organ transplantation. However, its exact mode of antitumor action remains unknown. The present study used the B16-F10 (B16) murine melanoma model to explore the antitumor mechanism of rapamycin, and it was revealed that rapamycin reduced B16 cell viability *in vitro* and *in vivo*. In addition, *in vitro* and *in vivo*, the results of western blotting showed that rapamycin reduced Bcl2 expression, and enhanced the protein expression levels of cleaved caspase 3 and Bax, indicating that it can induce the apoptosis of B16 melanoma cells. Furthermore, the results of cell cycle analysis and western blotting showed that rapamycin induced B16 cell cycle arrest in the G_1 phase, based on the reduction in the protein expression levels of CDK1, cyclin D1 and CDK4, as well as the increase in the percentage of cells in G_1 phase. Rapamycin also significantly increased the number of autophagosomes in B16 melanoma cells, as determined by transmission electron microscopy. Furthermore, the results of RT-qPCR and western blotting showed that rapamycin upregulated the protein expression levels of microtubule-associated protein light chain 3 (LC3) and Beclin-1, while downregulating the expression of p62 *in vitro* and *in vivo*, thus indicating that rapamycin could trigger cellular autophagy. The present study revealed that rapamycin in combination with chloroquine (CQ) further increased LC3 expression compared with that in the CQ group, suggesting that rapamycin induced an increase in autophagy in B16 cells. Furthermore, the results of western blotting showed that rapamycin blocked the phosphorylation of p70 ribosomal S6 kinase (p70-S6k) and mammalian target of rapamycin (mTOR) proteins *in vitro* and *in vivo*, thus suggesting that rapamycin may exert its antitumor effect by inhibiting the phosphorylation of the mTOR/p70-S6k pathway. In conclusion, rapamycin may inhibit tumor growth by inducing cellular G_1 phase arrest and apoptosis. In addition, rapamycin may exert its antitumor effects by inducing the autophagy of B16 melanoma cells *in vitro* and *in vivo*, and the mTOR/p70-S6k signaling pathway may be involved in this process.

Introduction

Currently, most end-stage disorders can be successfully treated by organ transplantation, including heart transplantation, liver transplantation and kidney transplantation (1-3). However, recipients of organ transplants require a lengthy course of immunosuppressive therapy, which may increase the frequency of malignancies (1,4). Notably, previous studies have shown that patients who have undergone organ transplantation have a 2-8 times higher incidence of malignant melanoma than those who are immunocompetent (5-8). Post-transplantation malignancy seriously affects the quality of life of patients, and it is one of the main causes of death among transplant recipients (9). A previous study showed that of the 126,474 deaths in the United States after solid organ transplants between 1987 and 2018, 13% were due to cancer (10). Therefore, the search for drugs that have both anti-rejection and antitumor properties is essential.

Rapamycin, a macrolide antibiotic, exerts its immunosuppressive function mainly by acting on mammalian target of rapamycin (mTOR) (11). Unlike calcineurin inhibitors, which may increase tumor incidence after transplantation (12), rapamycin can be applied to inhibit tumor spread and recurrence following organ transplantation (13-15). Rapamycin has been shown to inhibit the growth of a mouse hepatocellular carcinoma xenograft model by targeting STAT3 and affecting

Correspondence to: Professor Chang Gao or Professor Hanyi Jiao, Department of Basic Medicine and Life Sciences, Hainan Medical University, 3 Academy Road, Haikou, Hainan 570100, P.R. China
E-mail: gaochang@hainmc.edu.cn
E-mail: jiaohanyi@hainmc.edu.cn

*Contributed equally

Key words: rapamycin, B16 melanoma cells, autophagy, apoptosis, cell cycle, mTOR/p70-S6k signaling pathway

c-Myc, in addition to inhibiting angiogenesis in an *in vivo* CT-26 cell model of liver metastasis (16,17). In addition, rapamycin has been reported to inhibit tumor growth in a mouse model of breast cancer established using the MC4-L2 cell line, and to inhibit the viability of kaposiform hemangioendothelioma primary cells and human osteosarcoma MG-63 cells by inducing autophagy and apoptosis (18-20). For different tumor types, rapamycin may act in diverse ways. Malignant melanoma is easily metastasized and has a poor prognosis once it has progressed to an advanced stage (21). Research has found that the median duration from transplant to melanoma diagnosis in the individuals who have undergone lung and heart transplants is 2.5 years (22). Some studies have shown that rapamycin inhibits the growth of A375 malignant melanoma in an *in vitro* model (23,24). However, the mechanism of action of the effects of rapamycin on malignant melanoma remains to be explored.

The present study aimed to examine the effects of rapamycin on cell viability, cell apoptosis, cell cycle progression, and cellular autophagy and related signaling pathways in B16-F10 (B16) murine melanoma cells. Additionally, *in vivo* experiments were performed to verify the anti-melanoma effect of rapamycin.

Materials and methods

Cell culture. Mouse B16 melanoma cells purchased from EK Biosciences GmbH were cultured in Gibco Dulbecco's modified Eagle's medium supplemented (cat. no. C1995500BT) with 1% penicillin-streptomycin and 10% gibco fetal bovine serum (cat. no. 10099-141) (Thermo Fisher Scientific, Inc.) in an incubator at 37˚C and 5% CO_2. The medium was changed every 1-2 days, and when the cells covered 90% of the culture flasks, they were trypsinized and passaged. All cell lines tested negative for *Mycoplasma* contamination.

Reagents and drugs. The Annexin V-FITC/PI double staining cell apoptosis detection kit (cat. no. BD556547) was purchased from BD Biosciences. Mouse GAPDH monoclonal antibody (cat. no. 60004-1-Ig), mouse Beclin-1 monoclonal antibody (cat. no. 66665-1-Ig), mouse caspase 3/p17/p19 monoclonal antibody (cat. no. 66470-2-Ig), mouse Bax monoclonal antibody (cat. no. 60267-1-Ig), mouse Bcl2 monoclonal antibody (cat. no. 68103-1-Ig), mouse cyclin D1 monoclonal antibody (cat. no. 60186-1-Ig), mouse CDK4 monoclonal antibody (cat. no. 66950-1-Ig), mouse CDK6 monoclonal antibody (cat. no. 66278-1-Ig), mouse CDK2 monoclonal antibody (cat. no. 60312-1-Ig), rabbit cyclin E1 polyclonal antibody (cat. no. 11554-1-AP), rabbit microtubule-associated protein light chain 3 (LC3) polyclonal antibody (cat. no. 14600-1-AP), goat anti-rabbit IgG-HRP (cat. no. SA00001-2) and goat anti-mouse IgG-HRP (cat. no. SA00001-1) antibodies were purchased from ProteinTech Group, Inc. Rabbit sequestosome 1/p62 (cat. no. AF5384), mTOR (cat. no. AF6308), p70 ribosomal S6 kinase (p70-S6k; cat. no. AF6226), eukaryotic initiation factor 4E-binding protein (4E-BP1; cat. no. AF6432), phosphorylated (p)-mTOR (cat. no. AF3308), p-p70-S6k (cat. no. AF3228) and p-4E-BP1 (cat. no. AF3830) polyclonal antibodies were purchased from Affinity Biosciences. Thiazolyl Blue (MTT; cat. no. HY-15924), rapamycin (cat. no. HY-10219) and chloroquine (CQ; cat. no. HY-17589A), an autophagy inhibitor that can block the degradation of LC3 and p62 by inhibiting the fusion of autophagosomes and lysosomes, were purchased from MedChemExpress. Rapamycin was configured with DMSO into 10^0, 10^1, 10^2, 10^3, 10^4, 10^5, 10^6, 10^7 and 10^8 nM concentrated reservoirs (later diluted), and stored frozen at -20 or -80˚C for *in vitro* cell experiments. For *in vivo* animal studies, the drug solution was prepared in anhydrous ethanol and phosphate-buffered saline (PBS) at a concentration of 1 mg/ml and stored at -20˚C, ready to use.

In vitro cell viability assay. Cell suspensions made from logarithmic cells were inoculated into 96-well culture plates (20,000 cells/well). Solubilized rapamycin solution (final drug concentrations, 10^{-3}, 10^{-2}, 10^{-1}, 10^0, 10^1, 10^2, 10^3, 10^4 and 10^5 nM) was added. After 48 h at 37˚C, 20 μl MTT working solution (5 g/l) was added to each well and the cells were incubated at 37˚C for 4 h. After discarding the supernatant, the purple formazan crystals were solubilized with 150 μl DMSO. Finally, the optical density was measured at 492 nm using a plate reader (Multiskan FC; Thermo Fisher Scientific, Inc.).

Cell apoptosis assay. B16 cells pretreated with different concentrations (0, 0.1, 1, 10 and 100 nM) of rapamycin for 48 h at 37˚C were collected. The supernatant was collected from the 6-well plate, and ~$1x10^5$ cells/well were digested with 0.25% EDTA-free trypsin after washing with PBS. After termination of digestion, the cells were centrifuged at 500 x g for 5 min at 4˚C. The cells were then washed twice with PBS, 500 μl binding buffer was added, and the cells were incubated with Annexin V-FITC (5 μl) and PI (5 μl) at room temperature for 15 min in the dark. Finally, the stained cells were detected by flow cytometry (NovoCyte 2040R with FlowJo v10.9; ACEA Bioscience, Inc.) within 2 h (25).

Cell cycle analysis. The culture fluid was collected from the cells into a centrifuge tube and set aside for termination of digestion, and $1x10^5$ cells/well were digested with 0.25% trypsin after PBS rinsing. After the cells were collected into a centrifuge tube, they were centrifuged at 4˚C for 3 min at 1,000 x g. The cells were washed twice with pre-cooled PBS and added to 1 ml pre-cooled 70% ethanol. The cells were gently aspirated and blown with a spiking gun to prevent clumps, then mixed and fixed at 4˚C for 12 h. The cells were centrifuged for a further 3 min at 1,000 x g and 4˚C. The supernatant was then aspirated and washed once with PBS. Subsequently, 500 μl staining buffer (Cell Cycle Kit; cat. no. C1052; Beyotime Institute of Biotechnology), 25 μl PI staining solution (20 X) and 10 μl RNase A (50X) was added to each sample. After incubation at room temperature for 30 min, PI staining was examined by flow cytometry (NovoCyte 2040R with FlowJo v10.9; ACEA Bioscience, Inc.).

Reverse transcription-quantitative PCR (RT-qPCR). Total RNA was extracted from the B16 cells using TRIzol® reagent (Invitrogen; Thermo Fisher Scientific, Inc.), and the A260/A280 of total RNA in each group was determined. A PrimeScript® RT Reagent Kit (cat. no. RR047A; Takara Bio, Inc.) was used to reverse transcribe RNA into cDNA. qPCR was performed on a real-time PCR detection instrument (Light Cycler 480II;

Table I. Sequences of primers used in the present study.

Gene	Primer sequence (5'-3')	Accession no.
Mouse GAPDH	F: GGTTGTCTCCTGCGACTTCA R: TGGTCCAGGGTTTCTTACTCC	NM_008084
Mouse LC3 II	F: CAAGCCTTCTTCCTCCTGGTGAATG R: CCATTGCTGTCCCGAATGTCTCC	NM_025735.3
Mouse Beclin-1	F: GACGAACTCAAGAGTGTGGAGAACC R: AGATGTGGAAGGTGGCATTGAAGAC	NM_001359819.1
Mouse p62	F: TTCCAGCACAGGCACAGAAGAC R: TCCCACCGACTCCAAGGCTATC	NM_001290769.1

F, forward; LC3, microtubule-associated protein light chain 3; R, reverse.

Roche Diagnostics) with a TB Green® Premix Ex Taq™ II (Tli RNaseH Plus) cat. no. RR820A; Takara Bio, Inc.) following standard procedures. The thermal cycling conditions were as follows: 95˚C for 30 sec of pre-denaturation; followed by 40 cycles at 95˚C for 5 sec and 60˚C for 30 sec; and a final incubation at 95˚C for 5 sec and 60˚C for 1 min. Finally, the reaction was cooled to 50˚C in 30 sec. The relative expression levels of autophagy-related genes were quantified using the $2^{-\Delta\Delta Cq}$ (26) method using GAPDH as a control. The mRNA expression levels were normalized to those of GAPDH. The primer sequences are shown in Table I.

Transmission electron microscopy (TEM). A total of 200,000 B16 cells per well were inoculated in 6-well culture plates and allowed to grow for 48 h. TEM was used to examine the morphology of B16 cells under 0, 1 and 10 nM rapamycin treatment for 48 h at 37˚C. Briefly, cells were immediately fixed in electron microscopy fixative (3% osmium tetroxide) for 2 h at 4˚C. After low-speed centrifugation for 3 min at 1,000 x g and 4˚C, they were rinsed three times with PBS (pH 7.4). Subsequently, the cells were dehydrated in a graded ethanol series, then permeabilized and embedded in acetone, and cut into 60-80 nm ultrathin sections. Sections were double-stained with uranium-lead (2% uranyl acetate saturated alcohol solution and 3% lead citrate, each for 15 min at room temperature 25˚C), and sections were dried at room temperature overnight. The sections were finally observed under TEM (HT7700; Hitachi, Ltd.) and images were collected for analysis.

Western blotting. Lysis buffer (cat. no. P0013B; Beyotime Institute of Biotechnology) containing 1 mM phenylmethanesulfonyl fluoride was used to extract total cellular or mouse tumor tissue proteins after treatment, and the bicinchoninic acid protein assay kit (cat. no. P0010; Beyotime Institute of Biotechnology) was used to measure protein concentration. SDS-PAGE at a 12% concentration was used to separate equal amounts of 0.8 μg/μl of protein samples, which were then transferred to PVDF membranes. The membranes were blocked for 15 min at room temperature in Rapid Blocking Solution (cat. no. P0252; Beyotime Institute of Biotechnology) and incubated for 2 h at room temperature with different primary antibodies against Beclin-1, LC3, p62, CDK1, caspase 3, Bax, Bcl2, cyclin D1, CDK4, CDK6, CDK2, cyclin E1, mTOR, p-mTOR, p70-S6k, p-p70S6k, 4E-BP1, p-4E-BP1 (dilution for all, 1:1,500) and GAPDH (dilution, 1:10,000). Membranes were then washed three times with PBS-0.05% Tween 20 and then incubated with HRP-coupled anti-rabbit or anti-mouse secondary antibodies (dilution of both, 1:10,000) for 2 h at room temperature. After PBS washing three times, protein bands were observed using a protein blotting assay kit (Applygen Technologies Inc.) with ultrasensitive enhanced chemiluminescence, and ImageJ software (National Institutes of Health) was used for semi-quantitative analysis of protein bands (27).

Animals. A total of 32 male C57BL/6 mice (age, 8 weeks; weight, 18 g) were purchased from the Guangdong Medical Laboratory Animal Centre. The mice were housed in an environment of 50-60% relative humidity and 21-25˚C, with an alternating light and dark cycle of 10/14 h. The mice had free access to clean water and food. The present study was performed in strict accordance with the recommendations in the Guide for the Care and Use of Laboratory Animals of the National Institutes of Health, Eighth Edition, 2010, and also complied with the ARRIVE guidelines and the AVMA euthanasia guidelines 2020 (28,29). The animal experiments were approved by the Ethics Committee of Hainan Medical University (Haikou, China; approval no. HYLL: 2022-227). All protocols were in accordance with the approved guidelines and regulations.

Model building and treatment. The abdominal hair of the mice was first shaved and sterilized, and then B16 cells ($1x10^6$ in 100 μl) were injected subcutaneously into the right abdomen of 8-week-old male C57BL/6 mice to establish a subcutaneous tumor transplantation model. These mice were randomly and evenly grouped into four groups (n=8 mice/group). To ensure successful inoculation, tumor length was regularly observed and recorded daily. To assess the inhibitory effect of rapamycin on B16 melanoma cells *in vivo*, the mice were treated with different doses of rapamycin (1, 1.5 and 2 mg/kg/day) for 12 days, and the control group was injected intraperitoneally with an equal amount of PBS. When the tumor diameter of control mice reached the execution criteria (15 mm), all mice were euthanized by intravenous

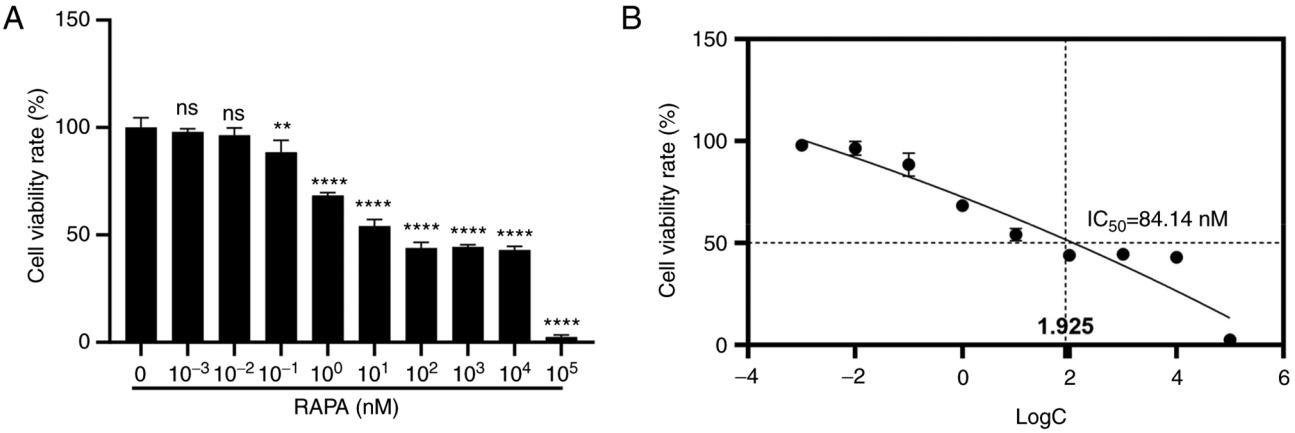

Figure 1. RAPA inhibits B16 cell viability *in vitro*. Cells were treated with RAPA for 48 h. (A) Cell viability was detected by MTT assay. (B) IC_{50} value of RAPA in B16 cells. Data are presented as the mean ± SD logC: for 10^{-3}, 10^{-2}, 10^{-1}, 10^{0}, 10^{1}, 10^{2}, 10^{3}, 10^{4} and 10^{5} nM take the logarithm of the base 10. (n=3). **P<0.01 and ****P<0.0001 vs. RAPA 0 nM group. B16, B16-F10; IC_{50}, half-maximal inhibitor concentration; ns, not significant; RAPA, rapamycin.

injection with an overdose of anesthetic (sodium pentobarbital, 150 mg/kg). Humane endpoints included malignancy, ulceration and necrosis. Tumors were removed and weighed. Tumor volume was measured as follows: Tumor volume (mm^3)=length x width x width/2.

Immunohistochemistry. The tumor tissues were fixed with 4% paraformaldehyde at room temperature for 24 h, paraffin embedded and cut into 4-μm sections. The sections were deparaffinized with xylene for 15 min twice and subsequently placed in 100, 95 and 80% ethanol, and sequentially rehydrated for 10 min. PBS-rinsed sections were immersed in 0.1 mol/l citrate (pH 6.0) and incubated for 15 min in a microwave oven for antigen repair. After the sections were cooled at room temperature for 10 min, incubation with 3% H_2O_2-PBS for 10 min at room temperature was used to eliminate endogenous peroxidase activity. Next, 5% BSA (cat. no. ST023; Beyotime Institute of Biotechnology) was applied at 37˚C to close the sections for 1 h. Subsequently, the sections were incubated with primary antibodies against the autophagy marker proteins LC3 (dilution, 1:200) and p62 (dilution, 1:200) at 37˚C for 1 h. PBS was used to replace the first antibodies in the blank control. After incubating with HRP-conjugated goat anti-rabbit (dilution, 1:300) at 37˚C for 20 min, tissue sections were stained with 3,3-diaminobenzidine and hematoxylin at room temperature for 5 min in turn. After being dehydrated and mounted, the tissues were observed under a fluorescence inverted microscope. Relative expression was assessed by measuring the average optical density of positive responses in each group using ImageJ software.

TUNEL fluorescence staining of paraffin-embedded tissue sections. The paraffin-embedded sections were deparaffinized and washed twice with PBS (5 min/wash). After shaking the sections dry, proteinase K working solution (cat. no. 11684795910; MilliporeSigma) was applied dropwise and the sections were incubated for 25 min at 37˚C before being washed twice with PBS. The sections underwent two PBS washes after being dried once more and treated with a membrane-breaking working solution for 10 min at room temperature. The sections were treated with a 50-μl 1:9 mixture of reagents TdT and Cy3-dUTP from the TUNEL kit (cat. no. 11684817910; Roche Diagnostics) at 37˚C for 1 h. After adding the DAPI staining solution and washing the sections three times in PBS (5 min/wash), they were maintained for 10 min at room temperature in the dark. After submerging the slides in PBS and shaking them three times (5 min each), the sections were blocked with an anti-fluorescence quenching sealing agent at 37˚C for 2 min once the sections had somewhat dried. Using a fluorescence microscope (DS-Fi3; Nikon Corporation), sections were examined and images were captured.

Statistical analysis. All experiments were conducted at least three times and data are presented as the mean ± standard deviation. GraphPad 9.5 software (Dotmatics) was used for statistical analysis. Multiple groups were compared using one-way ANOVA followed by Tukey's post hoc test. P<0.05 was considered to indicate a statistically significant difference.

Results

Rapamycin reduces the viability of B16 cells in vitro. To investigate the effects of rapamycin on B16 melanoma cell viability, the MTT assay was performed. B16 melanoma cells were treated with a range of rapamycin concentrations (0, 10^{-3}, 10^{-2}, 10^{-1}, 10^{0}, 10^{1}, 10^{2}, 10^{3}, 10^{4} and 10^{5} nM) for 48 h. As shown in Fig. 1A, rapamycin at a concentration of 10^{-1} nM significantly reduced the viability of B16 melanoma cells compared with that in the control group. In addition, the half-maximal inhibitory concentration of rapamycin in B16 cells was 84.14 nM (Fig. 1B).

Rapamycin induces the apoptosis of B16 cells in vitro. To investigate the possible mechanism by which rapamycin inhibits the viability of B16 cells, the present study examined the apoptosis of B16 cells following rapamycin treatment using flow cytometry. As shown in Fig. 2A and B, cell apoptosis was increased by rapamycin in the concentration range of 0.1-100 nM (10^{-7}-10^{-4} mM). In addition, rapamycin increased the protein expression levels of cleaved caspase 3 and Bax, and decreased the protein expression levels of Bcl2

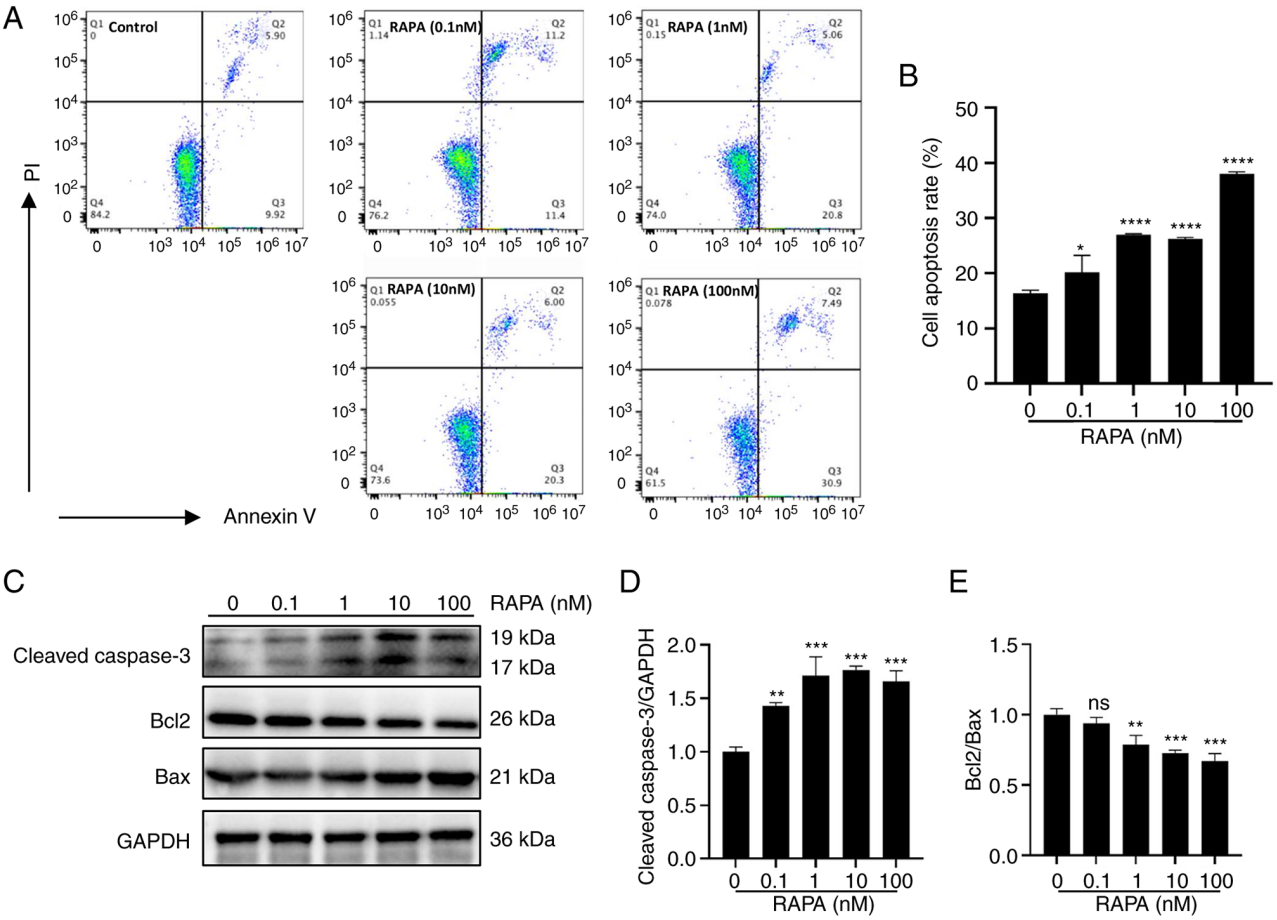

Figure 2. RAPA induces the apoptosis of B16 cells. B16 cells were treated with RAPA for 48 h. (A) Effects of RAPA on cell apoptosis were assessed through flow cytometry. (B) Statistical analysis of apoptosis rates for each group in (A). (C) Cleaved caspase 3, Bax and Bcl2 protein expression levels were detected by western blotting. (D) Relative expression of cleaved caspase 3 protein. (E) The ratio of Bcl2 to Bax protein expression. Data are presented as the mean ± SD (n=3). *P<0.05, **P<0.01, ***P<0.001 and ****P<0.0001 vs. RAPA 0 nM group. B16, B16-F10; ns, not significant; RAPA, rapamycin.

compared with those in the control group (Fig. 2C-E). These results indicated that rapamycin can induce the apoptosis of melanoma cells *in vitro*.

Rapamycin induces cell cycle arrest in B16 cells in vitro. After treating B16 cells with different concentrations of rapamycin, the cell cycle distribution of B16 cells was assessed using flow cytometry. As shown in Fig. 3A and B, rapamycin induced cell cycle arrest in B16 cells, with an increased proportion of cells in G_1 phase and a decreased proportion of cells in G_2/M phase compared with that in the control group. Furthermore, rapamycin reduced the protein expression levels of CDK1, cyclin D1 and CDK4, whereas it did not affect CDK6, cyclin E1 and CDK2 expression, compared with in the control group (Fig. 3C-I). These results suggested that rapamycin may induce B16 cell cycle arrest at G_0/G_1 phase.

Rapamycin induces autophagy in B16 cells. Autophagic vesicles observed by TEM are the gold standard for autophagy detection. In order to understand the effect of rapamycin on cellular autophagy, TEM was performed to observe the structure of the cells. The results revealed that the control cells had intact cell membranes, intact nuclear membranes, and a small number of autophagic vesicles and autophagic lysosomal structures (Fig. 4A). By contrast, B16 cells in the prominent 1 and 10 nM rapamycin groups had notably more autophagic vesicles and autophagic lysosomes than the cells in the control group. Moreover, cells in the 1 and 10 nM rapamycin groups exhibited marked cell membrane breaks and mitochondrial ridge breaks. Furthermore, at the gene and protein levels, rapamycin increased LC3 and Beclin-1 expression, and decreased p62 expression compared with that in the control group (Fig. 4B-H). To determine whether rapamycin enhanced autophagy, western blotting was used to detect the changes in LC3 and p62 expression following treatment with CQ (an autophagy inhibitor that blocks the degradation of LC3 and p62 by inhibiting the fusion of autophagosomes and lysosomes). Rapamycin in combination with CQ further increased LC3 and p62 expression compared with that in the CQ group, suggesting that rapamycin indeed induced an increase in autophagy in B16 cells (Fig. 4I-K).

Rapamycin inhibits the mTOR/p70-S6k signaling pathway in B16 cells. The mTOR/p70-S6k signaling pathway serves an important role in the regulation of autophagy, cell proliferation and cell survival in eukaryotic cells (30). To investigate the molecular mechanism underlying rapamycin-induced cellular autophagy in B16 cells, the expression and activation of important components of the mTOR signaling pathway, including p-mTOR, p-p70-S6k and p-4EBP1, were assessed after 48 h of rapamycin

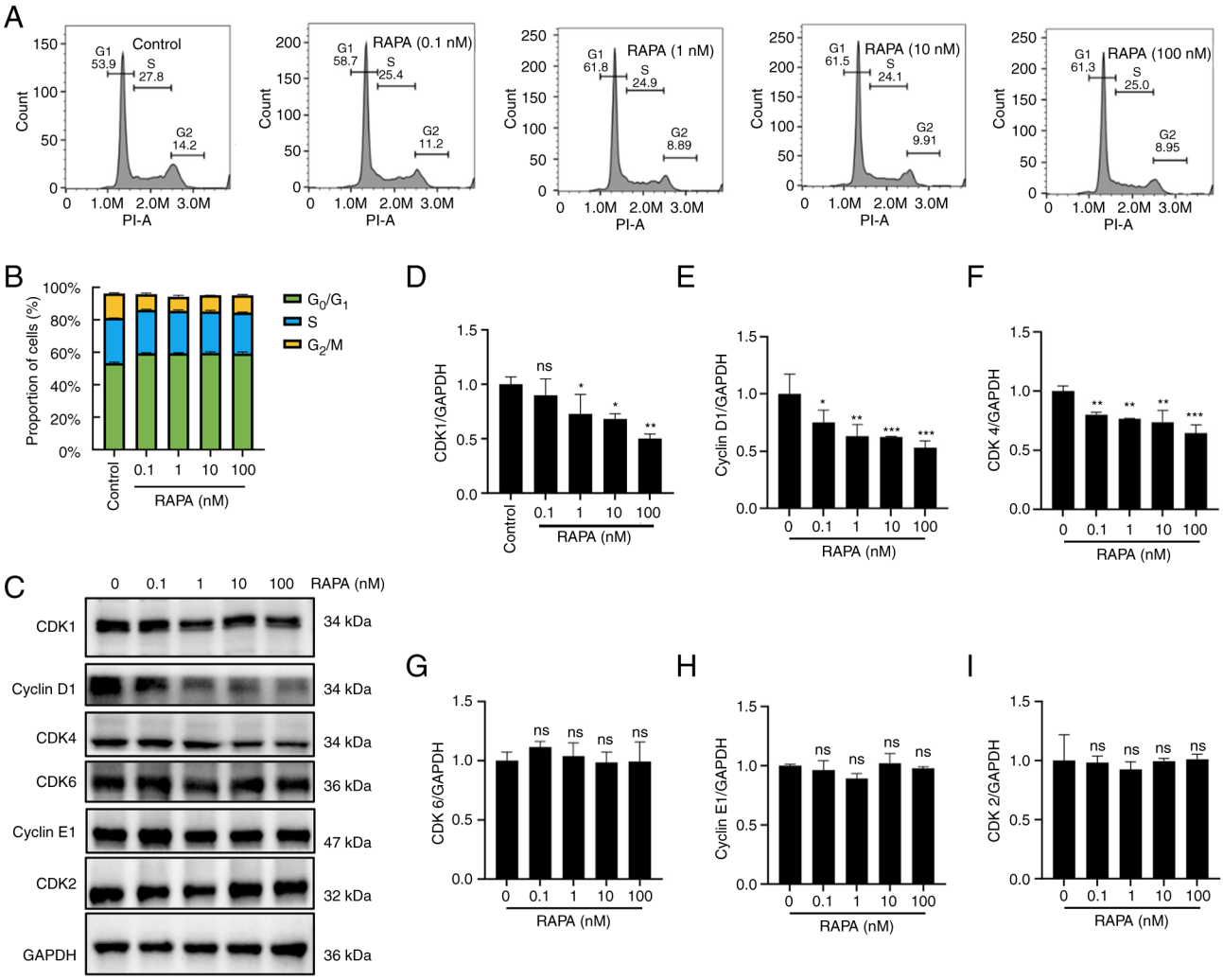

Figure 3. Effects of RAPA on the cell cycle progress of B16-F10 cells. (A) Cell cycle distribution was assessed by flow cytometry. (B) Results of statistical analysis of cell rates at different time periods for each group in (A). (C) CDK1, cyclin D1, CDK4, CDK6, cyclin E1 and CDK2 protein expression levels were detected by western blotting. Relative expression of (D) CDK1, (E) Cyclin D1, (F) CDK4, (G) CDK6, (H) Cyclin E1 and (I) CDK2 proteins. Data are presented as the mean ± SD (n=3). *P<0.05, **P<0.01 and ***P<0.001 vs. RAPA 0 nM group. ns, not significant; RAPA, rapamycin.

treatment. As shown in Fig. 5, the phosphorylation of mTOR and p70-S6k was downregulated by rapamycin compared with that in the control group, whereas there was no change in 4EBP1 phosphorylation. This result suggested that the mTOR/p70-S6k signaling pathway may be inhibited by rapamycin.

Rapamycin induces autophagy and inhibits the growth of melanoma B16 cells in the C57BL/6 mouse model. To determine whether rapamycin inhibits melanoma growth *in vivo*, B16 cells were subcutaneously injected into the abdomen of 8-week-old male mice, and rapamycin was administered at 1, 1.5 or 2 mg/kg/day. As shown in Fig. 6A-C, rapamycin at 1, 1.5 and 2 mg/kg/day effectively inhibited B16 melanoma growth compared with that in the control group. Western blotting results showed that the protein expression levels of LC3 II were increased, whereas the protein expression levels of p62 were decreased in rapamycin-treated tumors compared with those in the control group (Fig. 6D-F). Immunohistochemistry results showed an increase in the area of LC3 II-positive regions in rapamycin-treated tumors, along with a decrease in the area of p62-positive regions compared with that in the control group (Fig. 6G-I), which was consistent with the western blotting results. These findings suggested that rapamycin may induce B16 cell autophagy and suppress B16 melanoma growth *in vivo*.

Rapamycin induces apoptosis in mouse melanoma tumors. TUNEL fluorescent labeling and western blotting were performed to detect apoptosis in tumor tissues to examine whether rapamycin may trigger apoptosis in mice with melanoma *in vivo*. TUNEL immunofluorescence results showed that rapamycin promoted apoptosis of tumor cells in tumor tissues compared with that in the control group (Fig. 7A). The results of western blotting demonstrated that rapamycin induced a reduction in Bcl2 expression, and an increase in the expression levels of cleaved caspase 3 and Bax compared with those in the control group (Fig. 7B-D). These findings indicated that rapamycin may cause mouse melanoma tumor cells to undergo apoptosis.

Rapamycin inhibits the mTOR/p70-S6k/4E-BP1 signaling pathway in a mouse model. To determine if proteins

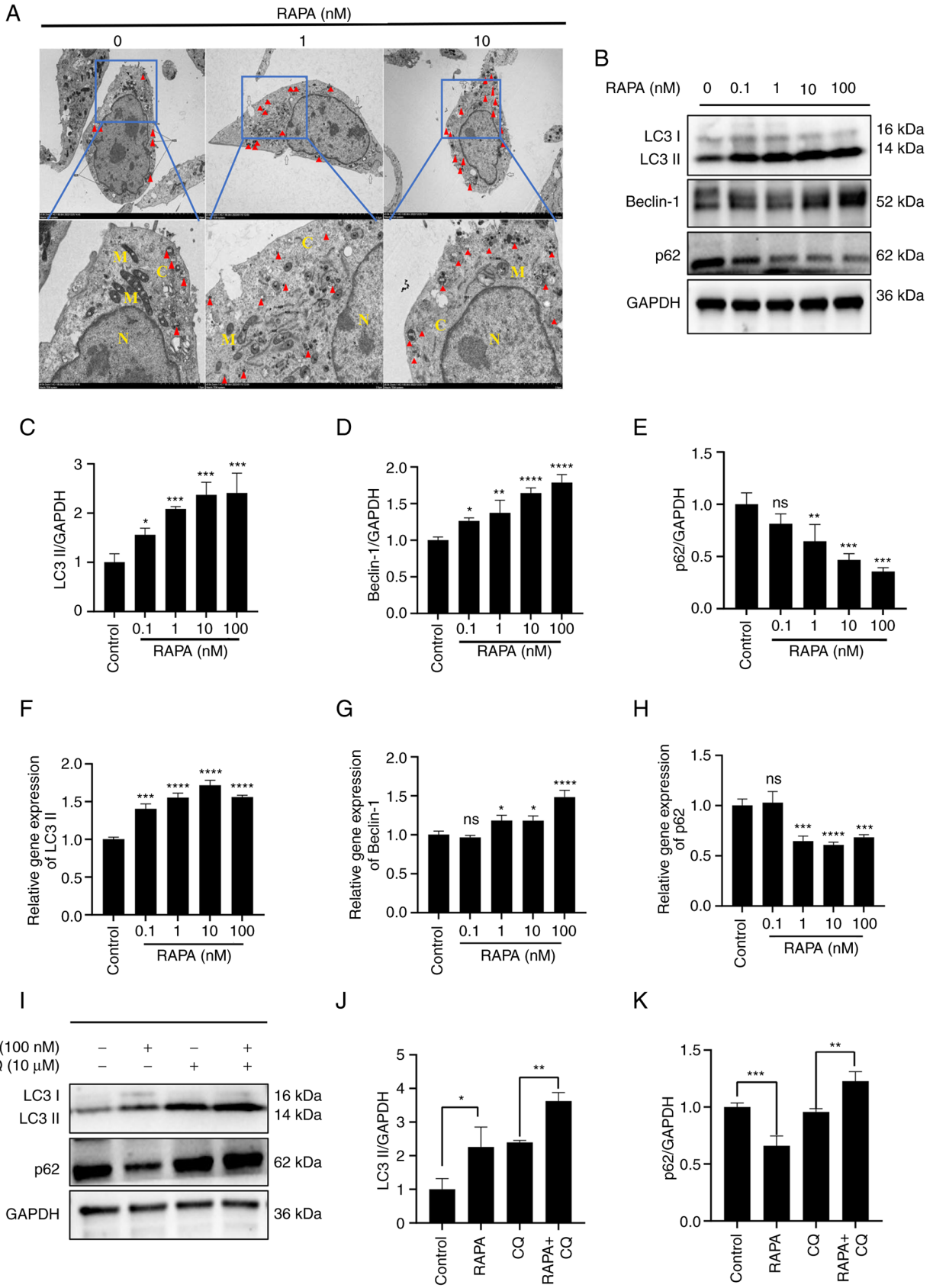

Figure 4. RAPA induces autophagy in B16 cells. (A) B16 cells were treated with 0, 1 and 10 nM RAPA for 48 h. The formation of autophagic vesicles was observed by transmission electron microscopy. M indicates mitochondrial structure, N the nucleus, C the cytoplasm, and red triangles indicate autophagic lysosomes. Magnification, x8,000; scale bar, 2.0 nm. (B) Expression levels of autophagy-related LC3, p62 and Beclin-1 in B16 cells were detected by western blotting. Relative expression of (C) LC3II, (D) Beclin-1 and (E) p62 proteins. Relative mRNA expression levels of (F) LC3 II, (G) Beclin-1 and (H) p62. (I) B16 cells were treated with rapamycin (100 nM) and/or CQ (10 μM) for 48 h. The protein expression levels of LC3 and p62 were detected by western blotting. (J) Relative expression of LC3II protein. (K) Relative expression of LC3II protein. Data are presented as the mean ± SD (n=3). *P<0.05, **P<0.01, ***P<0.001 and ****P<0.0001 vs. RAPA 0 nM group or as indicated. B16, B16-F10; CQ, chloroquine; LC3, microtubule-associated protein light chain 3; ns, not significant; RAPA, rapamycin.

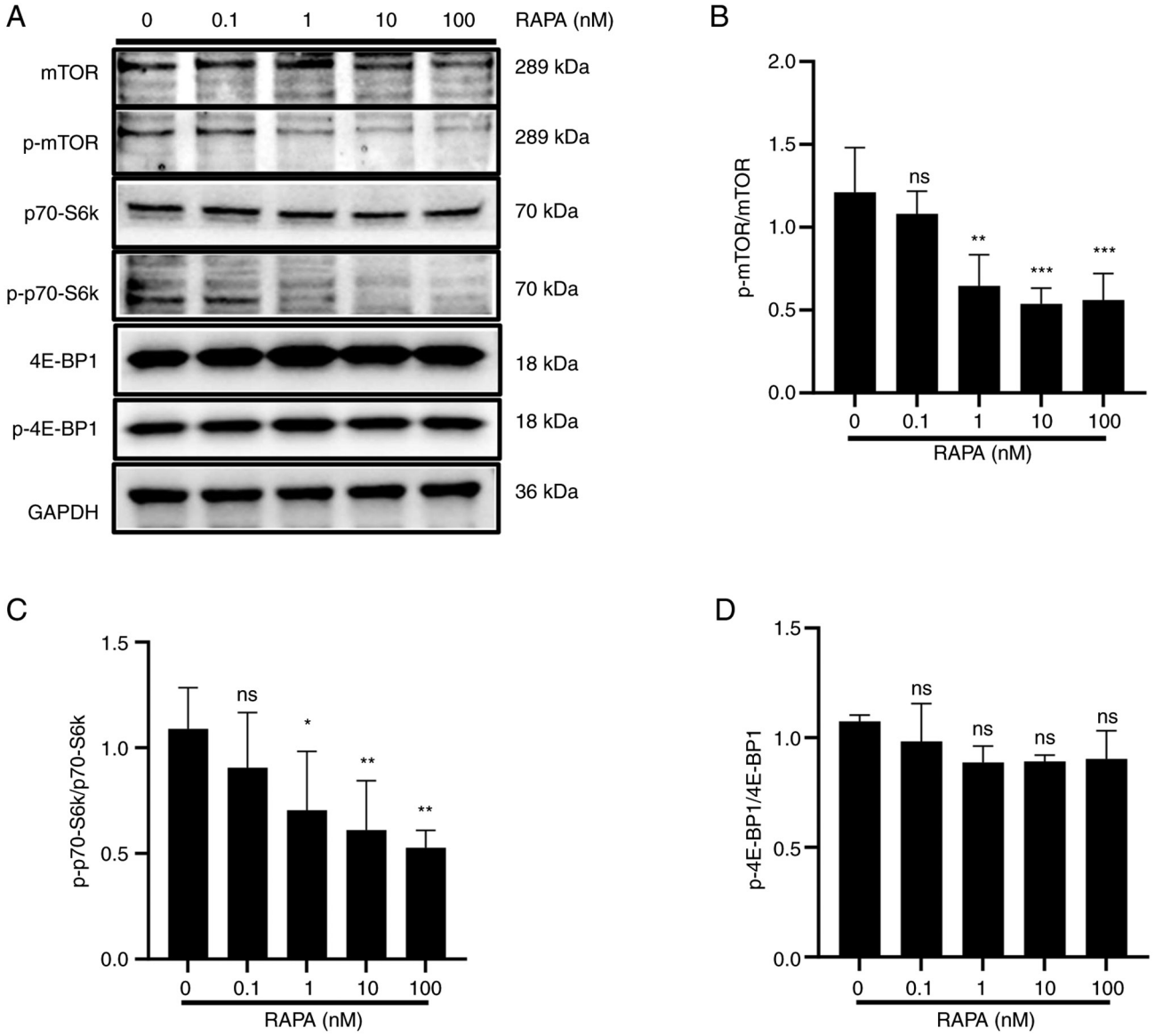

Figure 5. RAPA inhibits the mTOR/p70-S6k signaling pathway in B16 cells. B16 cells were treated with 0, 1, 10 and 100 nM RAPA for 48 h. (A) Western blotting results showed that RAPA inhibited the expression of p-mTOR and p-p70-S6k compared with in the control group. Statistical analysis of the (B) p-mTOR/mTOR ratio, (C) the p-p70-S6k/p70-S6k ratio and (D) the p-4E-BP1/4E-BP1 ratio at the protein level. Data are presented as the mean ± SD (n=3). *P<0.05, **P<0.01 and ***P<0.001 vs. RAPA 0 nM group. 4E-BP1, eukaryotic translation initiation factor 4e-binding protein 1; B16, B16-F10; mTOR, mammalian target of rapamycin; ns, not significant; p70-S6k, p70 ribosomal S6 kinase; p-, phosphorylated; RAPA, rapamycin.

associated with the mTOR/p70-S6k signaling pathway were altered in tumors, western blotting was performed. The administration of 1, 1.5 and 2 mg/kg/day rapamycin resulted in a decrease in the protein expression levels of p-mTOR, p-P70 S6k and p-4E-BP1 in comparison to those in the control group (Fig. 8A-D). These findings suggested that rapamycin can inhibit the mTOR/p70-S6k/4E-BP1 signaling pathway in tumor tissues.

Discussion

Rapamycin, a powerful and specific mTOR inhibitor, can specifically activate autophagy. Data from clinical studies have indicated that rapamycin has promising outcomes in the prevention or treatment of post-transplant tumor recurrence (13-15,31). However, the mechanism underlying the antitumor action of rapamycin has not yet been fully elucidated. The present study demonstrated that rapamycin may inhibit B16 melanoma cell growth by inducing autophagy in a C57BL/6 mouse model.

Melanoma is a malignant tumor, the frequency of which has quickly increased in recent decades (32). Melanoma is difficult to diagnose in the early stages and is often fatal once it has progressed to an advanced stage (33). Wang *et al* (24) reported that rapamycin can inhibit A375 melanoma cell growth. In the current study, it was confirmed that rapamycin could inhibit the viability of B16 melanoma cells both *in vivo* and *in vitro*.

The mechanism underlying the suppressive effects of rapamycin on B16 melanoma cells is not well understood. Cell cycle dysregulation is one of the key hallmarks of cancer cells. Numerous chemotherapeutic agents cause cell cycle arrest and promote apoptosis to stop the growth of human glioblastoma

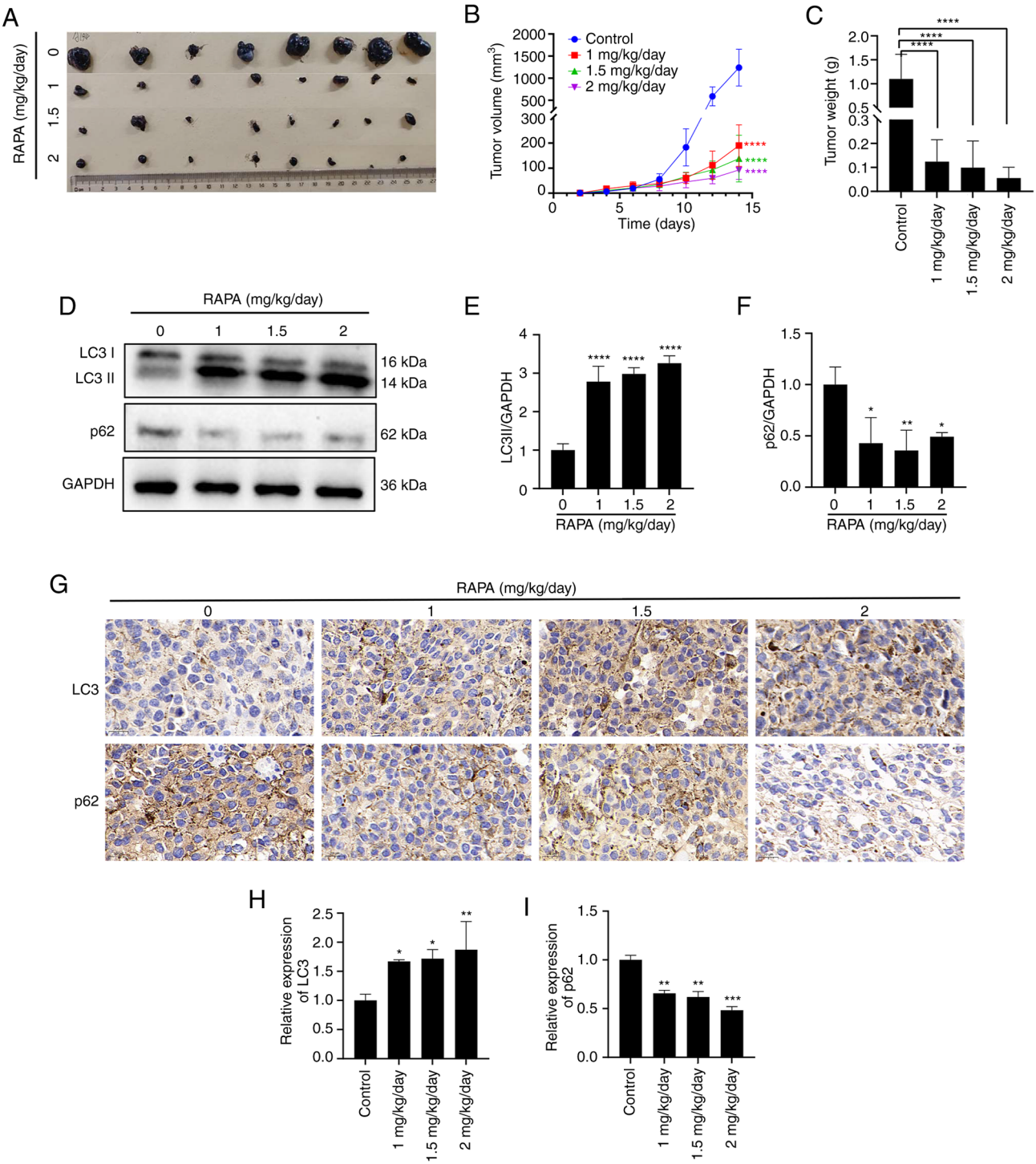

Figure 6. RAPA induces autophagy and inhibits growth of B16-F10 melanoma cells *in vivo*. (A) On day 14 of tumor growth, the mice were executed and the tumors were collected and photographed (n=8 mice per group). (B) Tumor volumes were measured using Vernier calipers and were calculated every day. (C) Tumor weight was measured. Data are presented as the mean ± SD (n=8). (D) Relative protein expression levels of LC3 and p62 were detected in tumors by western blotting. (E) Relative expression of LC3 II protein in tumor tissues. (F) Relative expression of p62 protein in tumor tissues. (G) Expression levels of LC3 and p62 in each group were detected by immunohistochemistry (magnification, x40; scale bar, 20 μm. (H) Statistical analysis of the area of LC3 protein-positive regions. (I) Statistical analysis of the area of p62 protein-positive regions. Data are presented as the mean ± SD (n=3). *P<0.05, **P<0.01, ***P<0.001 and ****P<0.0001 vs. RAPA 0 mg/kg/day group. LC3, microtubule-associated protein light chain 3; RAPA, rapamycin.

and other types of cancer cells (34,35). Furthermore, rapamycin has been shown to induce cell cycle arrest in the G_1 phase and promote apoptosis in several cancer types, including renal cancer cells and glioma cells (36,37). The present results revealed that rapamycin treatment increased the proportion of B16 cells in the G_1 phase, and decreased the protein expression levels of CDK1, cyclin D1 and CDK4. We therefore hypothesized that rapamycin-induced cell cycle arrest may be one of the mechanisms that inhibits the viability of B16 cells.

Induction of apoptosis is key in the suppression of tumors. Rapamycin is a classic autophagy inducer, which is able to induce autophagy in most vital cells (38-41). However, some

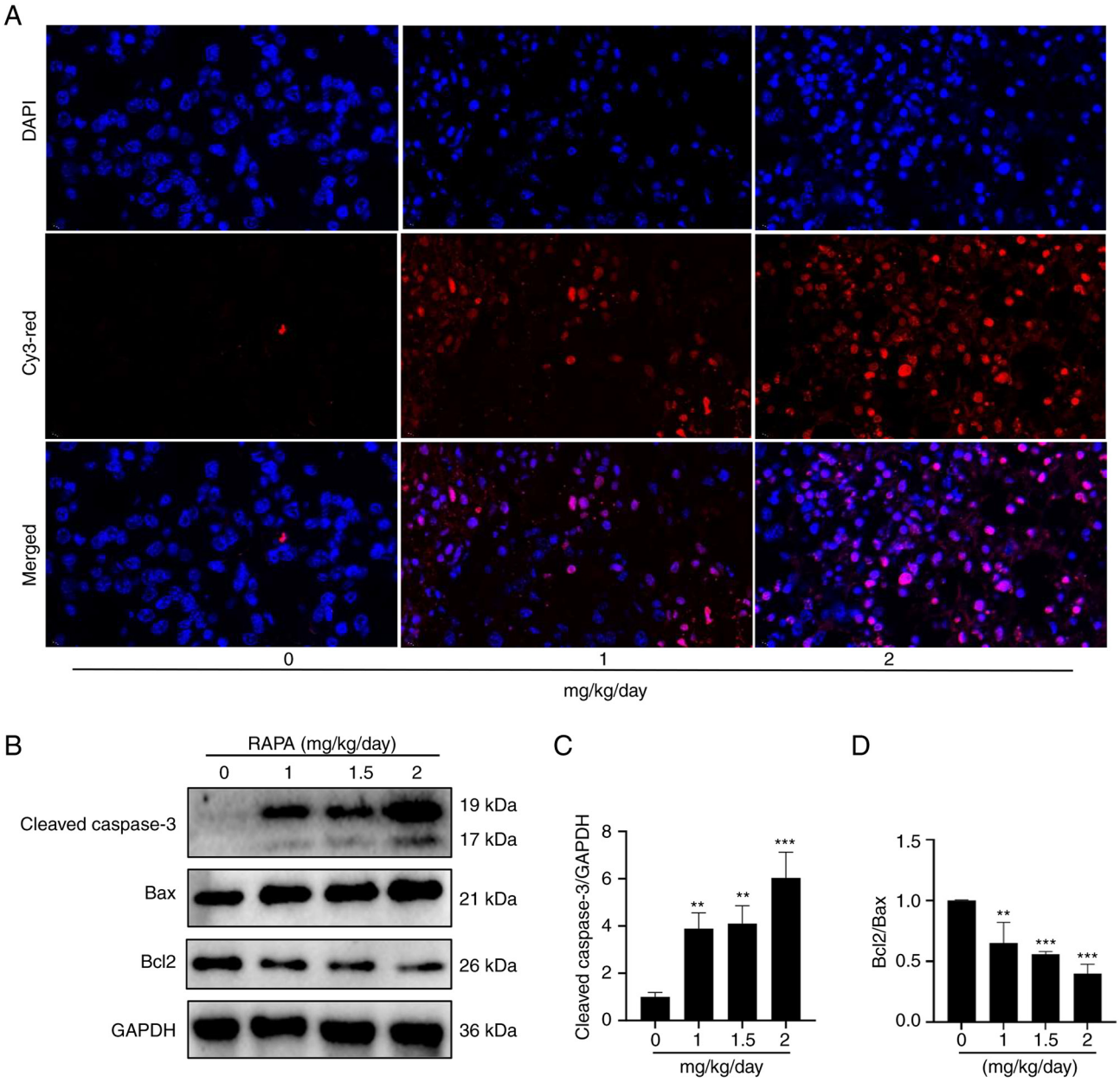

Figure 7. RAPA induces apoptosis in tumors. (A) TUNEL fluorescence staining of tumor cell death detected by fluorescence microscopy (magnification, x100; scale bar, 10 μm). (B) Western blotting results showed that RAPA significantly increased the expression levels of cleaved caspase 3 and Bax, and decreased the expression levels of Bcl2. (C) Results of relative expression analysis of Cleaved caspase 3 protein in tumor tissues. (D) Statistical analysis of the ratio of the protein Bcl2/Bax in tumor tissues. Data are presented as the mean ± SD (n=3). **P<0.01 and ***P<0.001 vs. RAPA 0 mg/kg/day group. RAPA, rapamycin.

studies have also found that it can induce the apoptosis of certain types of cells, including Kaposiform hemangioendothelioma primary cells, human MG-63 osteosarcoma cells and SHSY5Y neuroblastoma cells (19,20,42,43). It has been shown that rapamycin induces B16 cell apoptosis in a lung metastasis model (44). The present study showed that rapamycin can cause B16 cells to undergo apoptosis both *in vivo* and *in vitro* by increasing the expression levels of the apoptotic proteins cleaved caspase 3 and Bax. This may be one of the underlying mechanisms by which rapamycin prevents B16 cell viability.

The relationship between autophagy and cancer has long been discussed, and there exists an 'autophagy paradox'. On the one hand, autophagy breaks down cellular components that may supply substrates for biogenesis, including cancer cells. On the other hand, if this process is overactive, cells may excessively degrade and eventually die, including cancer cells (45). Studies have shown that in breast cancer, osteosarcoma and pancreatic cancer, inducing autophagy can significantly inhibit growth and proliferation (46-48). The present results also showed that rapamycin induced B16 melanoma cell autophagy and suppressed cell viability in a dose-dependent manner. LC3 and p62 proteins are two important indicators of autophagy. LC3 is the only mammalian autophagy-related protein known to be uniquely associated with autophagosomes and is positively correlated with the amount of autophagosomes. By contrast, the p62 protein is degraded after the formation of autophagic lysosomes and therefore its concentration is generally considered to be inversely correlated with

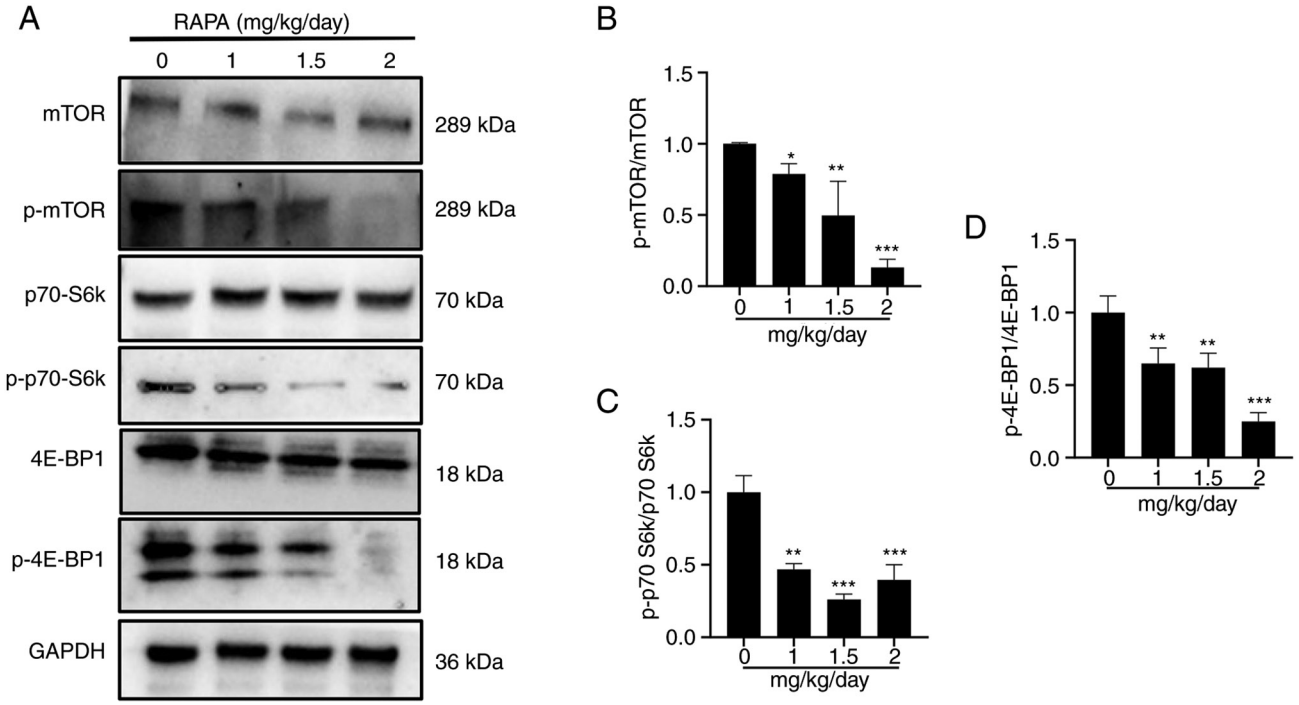

Figure 8. RAPA inhibits the mTOR/p70-S6k signaling pathway in tumors. Proteins were extracted from tumors. (A) Western blotting results showed that RAPA significantly inhibited the expression levels of p-mTOR, p-4E-BP1 and p-p70-S6k compared with in the control group in tumor tissues. Statistical analysis of the (B) p-mTOR/mTOR ratio, (C) the p-p70-S6k/p70-S6k and (D) the p-4E-BP1/4E-BP1 ratio in tumor tissues at the protein level. Data are presented as the mean ± SD (n=3). *P<0.05, **P<0.01 and ***P<0.001 vs. RAPA 0 mg/kg/day group. 4E-BP1, eukaryotic translation initiation factor 4e-binding protein 1; mTOR, mammalian target of rapamycin; p70-S6k, p70 ribosomal S6 kinase; p-, phosphorylated; RAPA, rapamycin.

autophagic activity (49). p62 has been used as a marker for the inhibition of autophagy, with its reduction indicating the activation of autophagy (50). The present study demonstrated that rapamycin promoted autophagy in mouse B16 melanoma cells *in vivo* and *in vitro*. We therefore hypothesized that cellular autophagy may be one of the main mechanisms by which rapamycin inhibits B16 cell viability.

The fact that autophagy is a highly dynamic, multi-step process that can be regulated at various levels. The ratio of the rate of autophagosome formation to the rate of destruction by fusion with lysosomes determines the number of autophagosomes that may be detected at any given time point (51). Therefore, an increase in LC3 II may indicate either an increase in autophagosome production brought on by the induction of autophagy or an obstruction of the subsequent autophagic stages, such as ineffective fusion or decreased autophagosome destruction (52). To confirm that rapamycin induced autophagy in B16 cells, changes in LC3 II expression were observed in response to CQ intervention. The results showed that rapamycin combined with CQ induced a further increase in LC3 II expression, which indicated that autophagy was further induced by rapamycin at the level of basal autophagy. This finding suggested that induction of autophagic kinetics is an important mechanism by which rapamycin inhibits the viability of B16 cells.

Dysregulated mTOR signaling is linked to cancer, metabolic dysregulation and aging. The mTOR and PI3K/AKT/mTOR complex 1 (mTORC1) signaling pathway are essential for the regulation of numerous fundamental cell processes, including protein synthesis, cell viability, metabolism, survival, catabolism and autophagy (53). Two essential molecules, p70-S6k and 4E-BP1, that support translation and protein synthesis are phosphorylated by mTORC1 to control protein synthesis (54). It has been reported that inhibition of the mTOR/p70-S6k signaling pathway suppresses cell viability, and induces apoptosis and autophagy (30). Rapamycin differentially inhibits S6Ks and 4E-BP1 to mediate cell type-specific repression of mRNA translation. (55,56). The present study revealed that rapamycin inhibited the phosphorylation of mTOR and p70-S6k in B16 cells in a dose-dependent manner both *in vivo* and *in vitro*. These findings indicated that rapamycin may slow down the viability of B16 cells by inhibiting the mTOR/p70-S6k pathway, inducing autophagy and/or inhibiting protein synthesis in B16 cells.

Overall, the present study demonstrated that rapamycin inhibited the viability of B16 cells *in vitro* and *in vivo* by inducing autophagy and apoptosis, and that inducing cell cycle arrest in the G_1 phase may also be one of the underlying mechanisms. In addition, rapamycin inhibited activation of the mTOR/p70-S6k signaling pathway, which controls protein synthesis and negatively regulates autophagy. Therefore, it was hypothesized that rapamycin may inhibit B16 cell viability by inducing autophagy and/or inhibiting protein synthesis through inactivation of the mTOR/p70-S6k signaling pathway; however, this hypothesis requires further study. In conclusion, the present study identified the possible mechanisms underlying rapamycin-induced tumorigenesis inhibition and provides a theoretical basis for rapamycin therapy of tumors in organ transplant recipients.

Acknowledgements

Not applicable.

Funding

This work was supported by grants from the National Natural Science Foundation of China (grant no. 81660270), Hainan Provincial Natural Science Foundation of China (grant nos. 823RC497, 823RC602 and 2019RC211), the Project of Nanhai Series of Talent Cultivation Program (grant no. 20192031), the Youth Science and Technology Talent Innovation Program of the Hainan Association for Science and Technology (grant no. QCXM201920), and the Key Discipline Project of Pathophysiology at Hainan Medical College (grant no. 04).

Availability of data and materials

The data generated in the present study may be requested from the corresponding author.

Authors' contributions

PW performed experiments, provided all figures and wrote the article. HZ analyzed data and designed experiments. KG, CL, BP and TF performed experiments and provided data for the paper. ShC and SiC analyzed the data and interpreted the results. HJ and CG contributed the central idea, designed the research, and provided reagents and funding. ShC and SiC confirm the authenticity of all the raw data. All authors read and approved the final manuscript.

Ethics approval and consent to participate

The animal experiments were approved by the Ethics Committee of Hainan Medical College (approval no. HYLL: -2022-227). All protocols were in accordance with the approved guidelines and regulations.

Patient consent for publication

Not applicable.

Competing interests

The authors declare that they have no competing interests.

References

1. Awad MA, Shah A and Griffith BP: Current status and outcomes in heart transplantation: A narrative review. Rev Cardiovasc Med 23: 11, 2022.
2. Hahn D, Hodson EM, Hamiwka LA, Lee VW, Chapman JR, Craig JC and Webster AC: Target of rapamycin inhibitors (TOR-I; sirolimus and everolimus) for primary immunosuppression in kidney transplant recipients. Cochrane Database System Rev 12: CD004290, 2019.
3. Yang LS, Shan LL, Saxena A and Morris DL: Liver transplantation: A systematic review of long-term quality of life. Liver Int 34: 1298-1313, 2014.
4. Geissler EK: Post-transplantation malignancies: Here today, gone tomorrow? Nat Rev Clin Oncol 12: 705-717, 2015.
5. Dzambova M, Secnikova Z, Jirakova A, Jůzlová K, Viklický O, Hošková L, Göpfertovà D and Hercogová J: Malignant melanoma in organ transplant recipients: Incidence, outcomes, and management strategies: A review of literature. Dermatol Ther 29: 64-68, 2016.
6. Park CK, Dahlke EJ, Fung K, Kitchen J, Austin PC, Rochon PA and Chan AW: Melanoma incidence, stage, and survival after solid organ transplant: A population-based cohort study in Ontario, Canada. J Am Acad Dermatol 83: 754-761, 2020.
7. Russo I, Piaserico S, Belloni-Fortina A and Alaibac M: Cutaneous melanoma in solid organ transplant patients. G Ital Dermatol Venereol 149: 389-394, 2014.
8. Zwald F, Carvajal RD, Walker J, Sawinski D and Al-Adra D: Analysis of malignant melanoma risk and outcomes in solid organ transplant recipients: Assessment of transplant candidacy and the potential role of checkpoint inhibitors. Clin Transplant 35: e14264, 2021.
9. Masuda Y, Mita A, Ohno Y, Kubota K, Notake T, Shimizu A and Soejima Y: De novo malignancy after adult-to-adult living donor liver transplantation: A single-center long-term experience. Transplant Proc 55: 952-955, 2023.
10. Wang JH, Pfeiffer RM, Musgrove D, Castenson D, Fredrickson M, Miller J, Gonsalves L, Hsieh MC, Lynch CF, Zeng Y, *et al*: Cancer mortality among solid organ transplant recipients in the United States during 1987-2018. Transplantation 107: 2433-2442, 2023.
11. Naik MG, Arns W, Budde K, Diekmann F, Eitner F, Gwinner W, Heyne N, Jürgensen JS, Morath C, Riester U, *et al*: Sirolimus in renal transplant recipients with malignancies in Germany. Clin Kidney J 14: 2047-2058, 2021.
12. Kulbat A, Richter K, Stefura T, Kołodziej-Rzepa M, Kisielewski M, Wojewoda T and Wysocki WM: Systematic review of calcineurin inhibitors and incidence of skin malignancies after kidney transplantation in adult patients: A study of 309,551 cases. Curr Oncol 30: 5727-5737, 2023.
13. Berenguer M, Burra P, Ghobrial M, Hibi T, Metselaar H, Sapisochin G, Bhoori S, Man NK, Mas V, Ohira M, *et al*: Posttransplant management of recipients undergoing liver transplantation for hepatocellular carcinoma. Working group report from the ILTS transplant oncology consensus conference. Transplantation 104: 1143-1149, 2020.
14. Kim M, Rhu J, Choi GS, Kim JM and Joh JW: Risk factors for poor survival after recurrence of hepatocellular carcinoma after liver transplantation. Ann Surg Treat Res 101: 28-36, 2021.
15. Rajendran L, Ivanics T, Claasen MP, Muaddi H and Sapisochin G: The management of post-transplantation recurrence of hepatocellular carcinoma. Clin Mol Hepatol 28: 1-16, 2022.
16. Guba M, Graeb C, Jauch KW and Geissler EK: Pro- and anti-cancer effects of immunosuppressive agents used in organ transplantation. Transplantation 77: 1777-1782, 2004.
17. Sun L, Yan Y, Lv H, Li J, Wang Z, Wang K, Wang L, Li Y, Jiang H and Zhang Y: Rapamycin targets STAT3 and impacts c-Myc to suppress tumor growth. Cell Chem Biol 29: 373-385. e376, 2022.
18. Rostamzadeh D, Haghshenas MR, Samadi M, Mojtahedi Z, Babaloo Z and Ghaderi A: Immunosuppressive effects and potent anti-tumor efficacy of mTOR inhibitor everolimus in breast tumor-bearing mice. Iran J Allergy Asthma Immunol 21: 287-299, 2022.
19. Wang Z, Han Q, Wang J, Yao W, Wang L and Li K: Rapamycin induces autophagy and apoptosis in Kaposiform hemangioendothelioma primary cells in vitro. J Pediatr Surg 57: 1274-1280, 2022.
20. Yu WX, Lu C, Wang B, Ren XY and Xu K: Effects of rapamycin on osteosarcoma cell proliferation and apoptosis by inducing autophagy. Eur Rev Med Pharmacol Sci 24: 915-921, 2020.
21. Cust AE and Scolyer RA: Melanoma in situ-getting the diagnosis and prognosis right. JAMA Dermatol 159: 699-701, 2023.
22. Puza CJ, Cardones AR and Mosca PJ: Examining the incidence and presentation of melanoma in the cardiothoracic transplant population. JAMA Dermatol 154: 589-591, 2018.
23. Bundscherer A, Hafner C, Maisch T, Becker B, Landthaler M and Vogt T: Antiproliferative and proapoptotic effects of rapamycin and celecoxib in malignant melanoma cell lines. Oncol Rep 19: 547-553, 2008.
24. Wang M, Xu Y, Wen GZ, Wang Q and Yuan SM: Rapamycin suppresses angiogenesis and lymphangiogenesis in melanoma by downregulating VEGF-A/VEGFR-2 and VEGF-C/VEGFR-3 expression. Onco Targets Ther 12: 4643-4654, 2019.
25. Jurisic V, Srdic-Rajic T, Konjevic G, Bogdanovic G and Colic M: TNF-α induced apoptosis is accompanied with rapid CD30 and slower CD45 shedding from K-562 cells. J Membr Biol 239: 115-122, 2011.
26. Livak KJ and Schmittgen TD: Analysis of relative gene expression data using real-time quantitative PCR and the 2(-Delta Delta C(T)) method. Methods 25: 402-408, 2001.

27. Scherbakov AM, Vorontsova SK, Khamidullina AI, Mrdjanovic J, Andreeva OE, Bogdanov FB, Salnikova DI, Jurisic V, Zavarzin IV and Shirinian VZ: Novel pentacyclic derivatives and benzylidenes of the progesterone series cause anti-estrogenic and antiproliferative effects and induce apoptosis in breast cancer cells. Invest New Drugs 41: 142-152, 2023.
28. Leary S, Underwood W and Anthony R: AVMA guidelines for the euthanasia of animals: 2020 edition. AVMA, Schaumburg, IL, 2020.
29. National Research Council (US) Committee for the Update of the Guide for the Care and Use of Laboratory Animals: Guide for the Care and Use of Laboratory Animals, 8th edition. National Academies Press (US), Washington, DC, 2011.
30. Yang B and Zhao S: Polydatin regulates proliferation, apoptosis and autophagy in multiple myeloma cells through mTOR/p70s6k pathway. Onco Targets Ther 10: 935-944, 2017.
31. Saber-Moghaddam N, Nomani H, Sahebkar A, Johnston TP and Mohammadpour AH: The change of immunosuppressive regimen from calcineurin inhibitors to mammalian target of rapamycin (mTOR) inhibitors and its effect on malignancy following heart transplantation. Int Immunopharmacol 69: 150-158, 2019.
32. Gruber P and Zito PM: Skin Cancer. In: StatPearls. StatPearls Publishing LLC, Treasure Island, FL, 2023.
33. Rubatto M, Sciamarrelli N, Borriello S, Pala V, Mastorino L, Tonella L, Ribero S and Quaglino P: Classic and new strategies for the treatment of advanced melanoma and non-melanoma skin cancer. Front Med (Lausanne) 9: 959289, 2022.
34. Tsai TH, Su YF, Tsai CY, Wu CH, Lee KT and Hsu YC: RTA dh404 induces cell cycle arrest, apoptosis, and autophagy in glioblastoma cells. Int J Mol Sci 24: 4006, 2023.
35. Zhao W, Zhang L, Zhang Y, Jiang Z, Lu H, Xie Y, Han W, Zhao W, He J, Shi Z, *et al*: The CDK inhibitor AT7519 inhibits human glioblastoma cell growth by inducing apoptosis, pyroptosis and cell cycle arrest. Cell Death Dis 14: 11, 2023.
36. Sabarwal A, Chakraborty S, Mahanta S, Banerjee S, Balan M and Pal S: A novel combination treatment with honokiol and rapamycin effectively restricts c-met-induced growth of renal cancer cells, and also inhibits the expression of tumor cell PD-L1 involved in immune escape. Cancers (Basel) 12: 1782, 2020.
37. Wang Z, Wang X, Cheng F, Wen X, Feng S, Yu F, Tang H, Liu Z and Teng X: Rapamycin inhibits glioma cells growth and promotes autophagy by miR-26a-5p/DAPK1 Axis. Cancer Manag Res 13: 2691-2700, 2021.
38. Bjedov I and Rallis C: The target of rapamycin signalling pathway in ageing and lifespan regulation. Genes (Basel) 11: 1043, 2020.
39. Gao G, Chen W, Yan M, Liu J, Luo H, Wang C and Yang P: Rapamycin regulates the balance between cardiomyocyte apoptosis and autophagy in chronic heart failure by inhibiting mTOR signaling. Int J Mol Med 45: 195-209, 2020.
40. Masaki N, Aoki Y, Obara K, Kubota Y, Bouvet M, Miyazaki J and Hoffman RM: Targeting autophagy with the synergistic combination of chloroquine and rapamycin as a novel effective treatment for well-differentiated liposarcoma. Cancer Genomics Proteomics 20: 317-322, 2023.
41. Ni Z, Li H, Mu D, Hou J, Liu X, Tang S and Zheng S: Rapamycin alleviates 2,4,6-trinitrobenzene sulfonic acid-induced colitis through autophagy induction and NF-κB pathway inhibition in mice. Mediators Inflamm 2022: 2923216, 2022.
42. Ozates NP, Soğutlu F, Lerminoglu F, Demir B, Gunduz C, Shademan B and Avci CB: Effects of rapamycin and AZD3463 combination on apoptosis, autophagy, and cell cycle for resistance control in breast cancer. Life Sci 264: 118643, 2021.
43. Kocoglu SS, Sunay FB and Akkaya PN: Effects of monensin and rapamycin combination therapy on tumor growth and apoptosis in a xenograft mouse model of neuroblastoma. Antibiotics (Basel) 12: 995, 2023.
44. Yang Z, Lei Z, Li B, Zhou Y, Zhang GM, Feng ZH, Zhang B, Shen GX and Huang B: Rapamycin inhibits lung metastasis of B16 melanoma cells through down-regulating alphav integrin expression and up-regulating apoptosis signaling. Cancer Sci 101: 494-500, 2010.
45. Guo JY, Teng X, Laddha SV, Ma S, Van Nostrand SC, Yang Y, Khor S, Chan CS, Rabinowitz JD and White E: Autophagy provides metabolic substrates to maintain energy charge and nucleotide pools in Ras-driven lung cancer cells. Genes Dev 30: 1704-1717, 2016.
46. Hashemi M, Paskeh MDA, Orouei S, Abbasi P, Khorrami R, Dehghanpour A, Esmaeili N, Ghahremanzade A, Zandieh MA, Peymani M, *et al*: Towards dual function of autophagy in breast cancer: A potent regulator of tumor progression and therapy response. Biomed Pharmacother 161: 114546, 2023.
47. Li J, Chen X, Kang R, Zeh H, Klionsky DJ and Tang D: Regulation and function of autophagy in pancreatic cancer. Autophagy 17: 3275-3296, 2021.
48. Ning B, Liu Y, Huang T and Wei Y: Autophagy and its role in osteosarcoma. Cancer Med 12: 5676-5687, 2023.
49. Jiang P and Mizushima N: LC3- and p62-based biochemical methods for the analysis of autophagy progression in mammalian cells. Methods 75: 13-18, 2015.
50. Zhang Z, Singh R and Aschner M: Methods for the detection of autophagy in mammalian cells. Curr Protoc Toxicol 69: 20 12 21-20 12 26, 2016.
51. du Toit A, Hofmeyr JS, Gniadek TJ and Loos B: Measuring autophagosome flux. Autophagy 14: 1060-1071, 2018.
52. Klionsky DJ, Abdelmohsen K, Ab A, Abedi MJ, Abeliovic H, Arozen AA, Adach H, Adams CM, Adams PD, Adeli K, *et al*: Guidelines for the use and interpretation of assays for monitoring autophagy (3rd edition). Autophagy 12: 1-222, 2016.
53. Popova NV and Jucker M: The role of mTOR signaling as a therapeutic target in cancer. Int J Mol Sci 22: 1743, 2021.
54. Burnett PE, Barrow RK, Cohen NA, Snyder SH and Sabatini DM: RAFT1 phosphorylation of the translational regulators p70 S6 kinase and 4E-BP1. Proc Natl Acad Sci USA 95: 1432-1437, 1998.
55. Choo AY, Yoon SO, Kim SG, Roux PP and Blenis J: Rapamycin differentially inhibits S6Ks and 4E-BP1 to mediate cell-type-specific repression of mRNA translation. Proc Natl Acad Sci USA 105: 17414-17419, 2008.
56. Li B, Zhou C, Yi L, Xu L and Xu M: Effect and molecular mechanism of mTOR inhibitor rapamycin on temozolomide-induced autophagic death of U251 glioma cells. Oncol Lett 15: 2477-2484, 2018.